Nanoparticle halos: A new colloid stabilization mechanism

Valeria Tohver*, James E. Smay*, Alan Braem†, Paul V. Braun*‡, and Jennifer A. Lewis*‡§

*Department of Materials Science and Engineering and ‡Beckman Institute and Frederick Seitz Materials Research Laboratory, University of Illinois at Urbana-Champaign, Urbana, IL 61801; and †Department of Chemical Engineering, Carnegie Mellon University, Pittsburgh, PA 15213

Edited by David Chandler, University of California, Berkeley, Berkeley, CA, and approved May 25, 2001 (received for review February 7, 2001)

A new mechanism for regulating the stability of colloidal particles has been discovered. Negligibly charged colloidal microspheres, which flocculate when suspended alone in aqueous solution, undergo a remarkable stabilizing transition upon the addition of a critical volume fraction of highly charged nanoparticle species. Zeta potential analysis revealed that these microspheres exhibited an effective charge buildup in the presence of such species. Scanning angle reflectometry measurements indicated, however, that these nanoparticle species did not adsorb on the microspheres under the experimental conditions of interest. It is therefore proposed that highly charged nanoparticles segregate to regions near negligibly charged microspheres because of their repulsive Coulombic interactions in solution. This type of nanoparticle haloing provides a previously unreported method for tailoring the behavior of complex fluids.

Colloidal suspensions enjoy widespread use in applications ranging from advanced materials to drug delivery. By tailoring interactions between colloidal particles, one can design stable fluids, gels, or colloidal crystals needed for ceramics processing (1), coating (2), direct write (3), photonic (4–9), and pharmaceutical (10, 11) applications. Long range, attractive van der Waals forces are ubiquitous and must be balanced by Coulombic, steric, or other repulsive interactions to engineer the desired degree of colloidal stability.

The self-organization of highly charged nanoparticles and their influence on the behavior of complex fluids in which they dwell has received scant attention. The traditional view is that small particles or other species (e.g., polyelectrolyte, polymer, or micelles) in solution can promote flocculation of stable colloidal suspensions via an entropic depletion interaction (12–15). The term ''depletion'' describes the exclusion of these smaller species from the gap region between colloidal particles that arises when their separation distance becomes less than the characteristic depletant size. The resulting concentration gradient between the gap region and bulk solution gives rise to an attractive force, whose magnitude scales with the volume fraction of smaller species, their charge, and the size ratio of large to small species (12, 15, 16). However, emerging theoretical work (17–19) suggests that charged species in solution may affect system stability through other self-organizing pathways. For example, charged nanoparticles have been predicted to segregate to regions surrounding large *uncharged* colloids, especially in systems with high size asymmetry and many more small to large spheres (18). This segregation is driven solely by a Coulombic repulsion between smaller species in solution and occurs simply because the larger particles represent a big volume without charge. The key question we wish to explore is whether this type of haloing process can provide a mechanism for stabilizing colloidal species.

Here, we study the effects of highly charged nanoparticles on the behavior of negligibly charged colloidal microsphere mixtures, which undergo a remarkable transition from a colloidal gel → stable fluid → colloidal gel with increasing nanoparticle additions. We attribute the stabilizing transition to nanoparticle haloing around the microspheres, which serves to mitigate their long range van der Waals attraction. The system stability is ultimately reversed at higher nanoparticle volume fractions, where flocculation ensues because of entropic depletion forces (12–15, 20–22). Our observations open up a yet unexplored approach for stabilizing complex fluids.

Materials and Methods

Materials System. Uniform silica spheres (Geltech, Orlando, FL) with an average radius, a_{micro}, of 0.285 ± 0.01 or 0.590 ± 0.01 μm and a density of 2.25 g/cm^3 served as the colloidal microspheres. All experiments were carried out with the smaller microspheres unless otherwise noted. Hydrous zirconia nanoparticles (Nyacol Products, Ashland, MA) with an average radius, a_{nano}, of 3 nm (determined by x-ray scattering measurements), a reported radius range (23) of 0.5–11 nm, and a density (24, 25) of 3.65 g/cm^3 served as nanoparticle species. Such species are supplied in an acidic solution at a volumetric solids loading of 7.4%. Their refractive index was determined to be 1.98 from refractometry measurements (Abbe 3-L refractometer, Milton Ray, Rochester, NY) carried out on suspensions of varying nanoparticle volume fraction.

Sample Preparation. Concentrated suspensions were prepared by first adding an appropriate volume fraction of silica microspheres ($\phi_{\text{micro}} = 0.05$–$0.45$) to deionized water. The suspensions were stirred for ≈18 h with three intermittent sonications (model 550 sonic dismembrator) during the first 6 h. Nitric acid (Fisher Scientific) was then added to adjust the suspension pH to 1.5 ± 0.1. The suspension was resonicated followed by the addition of an appropriate volume fraction of nanoparticles ($\phi_{\text{nano}} = 10^{-6}$–$10^{-2}$). After stirring several hours, the suspension pH was readjusted to pH = 1.5 and sonicated a final time. Each sonication step consisted of 5 pulsed minutes (1 s on/off) at 20 kHz.

Zeta Potential Analysis. Zeta potential (ζ) measurements (ESA 9800, Matec Applied Science, Northboro, MA) were carried out on a concentrated silica suspension ($\phi_{\text{micro}} = 0.1$) as a function of varying pH in the absence of nanoparticle additions. The silica microspheres exhibited an isoelectric point at pH ≈2.5 and a ζ of roughly 1 mV at pH = 1.5. ζ measurements were also carried out on diluted silica suspensions with an initial $\phi_{\text{micro}} = 0.001$ and varying nanoparticle volume fraction in solution. In this set of experiments, we used an electrophoresis method (Laser Zee Meter model 501, Pen Kem, Bedford Hills, NJ) in which the microsphere mobility was directly observed as a function of applied voltage. The nanoparticle ζ could not be directly measured by electrosonic amplitude or electrophoretic techniques because of experimental limitations. Therefore, we estimated the nanoparticle ζ to be on the order of 70 mV from their reported effective charge Z^{eff} determined from titration studies

This paper was submitted directly (Track II) to the PNAS office.

§To whom reprint requests should be addressed. E-mail: jalewis@uiuc.edu.

The publication costs of this article were defrayed in part by page charge payment. This article must therefore be hereby marked "*advertisement*" in accordance with 18 U.S.C. §1734 solely to indicate this fact.

carried out by Peyre and coworkers (23), by using the approach outlined in ref. 26.

Nanoparticle Adsorption Measurements. The interaction of nanoparticle species with the colloidal silica microspheres was investigated by using a chemical analysis technique, in which the zirconium content, [Zr], in the supernatant solution was measured after microsphere sedimentation and compared with its known initial (bulk) value, [Zr_{bulk}], in solution. A series of binary suspensions ($\phi_{micro} = 0.1$ and varying $\phi_{nano} = 10^{-5}$–10^{-3}) were prepared and settled. Because of the effects of Brownian motion, only nanoparticles associated with the microspheres were removed from the supernatant solution during the sedimentation process. The volume fraction of nanoparticles associated with the settled microspheres was calculated from the difference of the initial [Zr_{bulk}] and supernatant [Zr] values, as determined by inductively coupled plasma analysis. In addition, scanning angle reflectometry (27, 28) was carried out to probe the adsorption behavior of nanoparticle species onto a model silica surface (i.e., an oxidized silicon wafer). Such experiments were conducted under pH conditions of 1.5 and 4.0. The nanoparticle solution was introduced into the experimental cell at $t = 15$ min.

Phase Behavior of Microsphere–Nanoparticle Mixtures. The phase behavior of binary mixtures of negligibly charged microspheres and highly charged nanoparticles were studied by two approaches. First, concentrated mixtures ($\phi_{micro} = 0.05$–0.45 and varying ϕ_{nano}) were visually inspected during sedimentation. In these experiments, a given volume of each suspension was placed in a graduated cylinder, which was then capped to minimize solvent loss. Initially, these samples were opaque because of the scattering of visible light from the colloidal microspheres. As the microspheres settled, a clear supernatant formed above the sedimented region. A rich variety of phase behavior was observed including the formation of colloidal gels that did or did not densify further via sedimentation and a homogeneous (binary) fluid that settled to form an iridescent colloidal crystal. Second, the microsphere distribution in dilute mixtures ($\phi_{micro} = 0.001$, $a_{micro} = 0.590$ μm, and varying ϕ_{nano}) was directly observed via optical microscopy by using a Zeiss Axiovert 100 inverted microscope equipped with a 100× oil lens. The larger microspheres were used in this experiment to provide enhanced image clarity.

Results

Nanoparticle Interactions with Colloidal Microspheres. The ζ data shown in Fig. 1*A* indicate that silica microspheres suspended near their isoelectric point adopt an effective charge of ≈65 mV with increasing nanoparticle volume fraction in solution. This plateau value, which occurs at $\phi_{nano} \approx 0.003$, is in remarkable agreement with the estimated ζ of the decorating nanoparticle species. Because the electrophoretic mobility of charged species is size independent, the microspheres and nanoparticles must move cooperatively to generate the observed charge buildup. This type of microsphere–nanoparticle movement is further supported by the data shown in Fig. 1*B*, which reflects the difference in nanoparticle content in the bulk versus supernatant solutions upon sedimentation of colloidal microspheres (and associated nanoparticles) from such mixtures. The presence of a significant fraction of nanoparticle species in the bulk solution, even at the lowest nanoparticle concentrations studied, suggests that strong nanoparticle adsorption is not likely. In fact, scanning angle reflectometry measurements revealed *no evidence* of nanoparticle adsorption on an oxidized silicon surface exposed to a nanoparticle solution ($\phi_{nano} = 10^{-3}$) at pH = 1.5 (see Fig. 2*A*). As a benchmark, we repeated these measurements at pH = 4, well above the isoelectric point of silica. Under such conditions, the silica surface is now negatively charged, whereas the nanoparticles remain highly positively charged. A strong Coulombic attraction therefore exists leading to the adsorption isotherm shown in Fig. 2*B*.

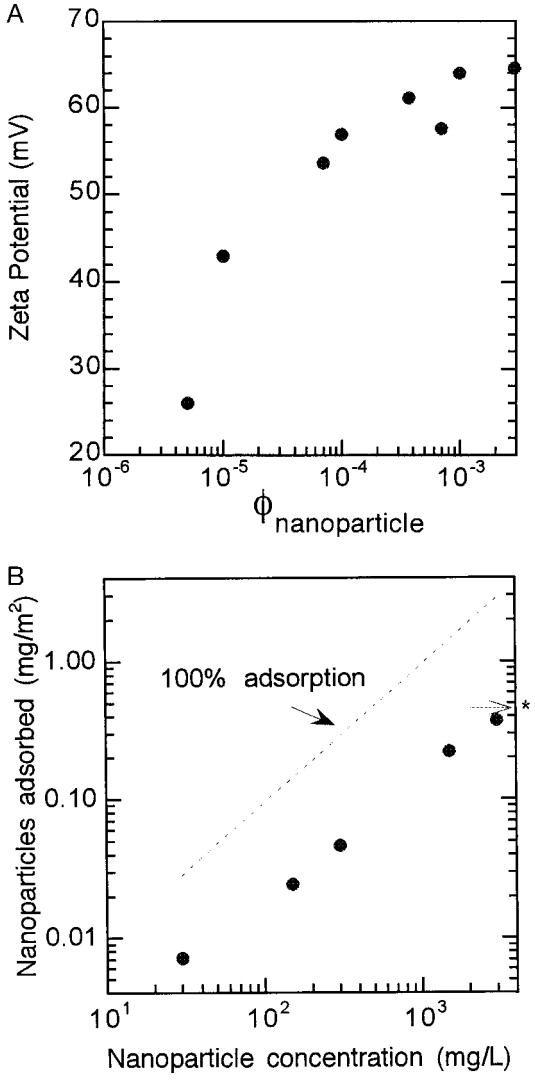

Fig. 1. (*A*) Semilog plot of microsphere zeta potential (ζ) as a function of nanoparticle volume fraction in pH 1.5 solution ($\phi_{micro} = 10^{-3}$; $\phi_{nano} = 0$–3×10^{-3}) and (*B*) nanoparticle adsorption on silica microspheres suspended in a pH 1.5 solution with $\phi_{micro} = 0.10$ and varying nanoparticle volume fraction. Chemical analysis of zirconium concentration, [Zr], in the supernatant solution was carried out upon microsphere sedimentation. Asterisk in *B* denotes expected nanoparticle adsorption of 0.46 mg/m^2 at a nanoparticle concentration of 3650 mg/liter.

Phase Behavior of Microsphere–Nanoparticle Mixtures. Fig. 3*A* depicts the phases observed for several mixtures of attractive microspheres and repulsive nanoparticles with a size ratio of 95. The data presented delineate three regions: (*i*) a colloidal gel composed of silica microspheres at nanoparticle volume fractions (ϕ_{nano}) below a lower critical value, $\phi^{L,C}$, (*ii*) a homogeneous fluid composed of stabilized silica microspheres and nanoparticles at intermediate nanoparticle volume fractions, $\phi^{L,C} \leq \phi_{nano} < \phi^{U,C}$, and (*iii*) a colloidal gel composed of silica microspheres at nanoparticle volume fractions (ϕ_{nano}) above an upper critical value, $\phi^{U,C}$. In the absence of nanoparticle species ($\phi_{nano} = 0$), the system began in a nonequilibrium state. Negligibly charged silica spheres underwent rapid flocculation (<60 s) to yield a colloidal gel. At $\phi_{micro} < 0.35$, weak gels

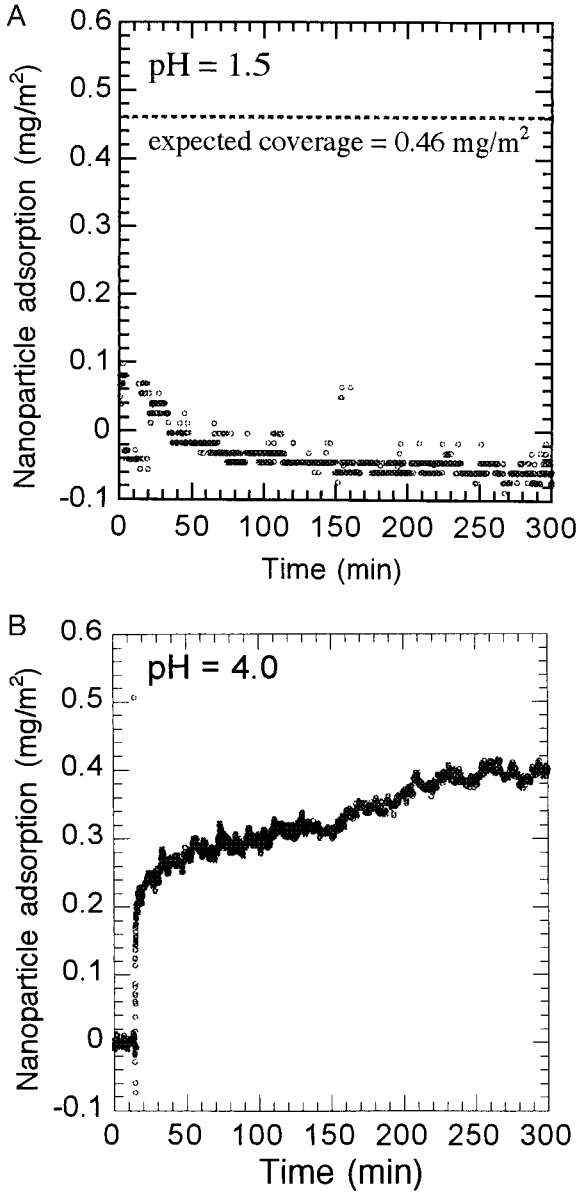

Fig. 2. Scanning angle reflectivity measurements of nanoparticle adsorption onto an oxidized Si wafer exposed to a nanoparticle ($\phi_{nano} = 10^{-3}$ or an equivalent concentration of 3650 mg/liter) in solution at pH = 1.5 (*A*) and pH = 4.0 (*B*).

formed that settled quickly, producing a loose-packed sediment and a clear supernatant. At $\phi_{micro} \geq 0.35$, stronger gels formed that could support their own mass and therefore did not undergo further densification in response to gravitational forces. Upon modest additions of nanoparticle species ($0 < \phi_{nano} < \phi^{L,C}$), the system remained in a nonequilibrium (gel) state. The silica microspheres flocculated to form a gel in coexistence with a nanoparticle fluid phase. Above a lower critical volume fraction ($\phi^{L,C}$) of nanoparticle species, a dramatic change in stability was observed. Many samples remained opaque for several days, until individual silica microspheres slowly settled yielding an iridescent (29), colloidal crystal. Such samples, considered fully stabilized, are denoted as the homogeneous fluid (F) phase in Fig. 3*A*. Above the upper critical volume fraction ($\phi^{U,C}$) of nanoparticles, this dramatic change in stability was reversed. For $\phi_{nano} \geq \phi^{U,C}$, the silica microspheres again flocculated, yielding a gel in coexistence with a nanoparticle fluid phase.

Optical micrographs and accompanying schematic illustrations of dilute microsphere–nanoparticle suspensions are depicted in Fig. 3*B*. These images illustrate the effect of nanoparticle additions on the structure of microspheres in solution. For $\phi_{nano} < \phi^{L,C}$, the microspheres were found to flocculate into a highly aggregated structure. For $\phi^{L,C} \leq \phi_{nano} < \phi^{U,C}$, the microspheres were suspended as discrete particles in solution. Finally, for $\phi_{nano} \geq \phi^{U,C}$, the microspheres were found to flocculate into a less aggregated structure. The accompanying schematic illustrations shown in Fig. 3 highlight the proposed distribution of nanoparticles in solution.

In control experiments on microsphere–nanoparticle mixtures with a larger size ratio of 197, both $\phi^{L,C}$ and $\phi^{U,C}$ were reduced at a given microsphere volume fraction, ϕ_{micro}. Similar phase behavior was observed, thus this stabilization mechanism appears to be general. For both mixtures, the initial microsphere network (or gel) was completely disrupted at nanoparticle additions above $\phi^{L,C}$, yielding individual microspheres suspended in a homogeneous fluid, as shown in Fig. 3*B*. As a hallmark of this stabilizing transition, the microspheres formed colloidal crystals under gravity-driven sedimentation. At nanoparticle additions above $\phi^{U,C}$, the microspheres reflocculated as shown in Fig. 3*B*.

Discussion

We propose that this remarkable stabilizing transition at intermediate nanoparticle volume fractions arises from a previously unreported colloidal stabilization mechanism, i.e., nanoparticle halo formation around the silica microspheres, whereas their reflocculation stems from traditional entropic depletion interactions. Here, we discuss evidence for these proposed mechanisms as well as the implications of our observations on complex fluid behavior.

Nanoparticle Haloing of Colloidal Microspheres. The segregation of highly charged nanoparticles to regions near negligibly charged colloidal microspheres has been predicted by the theoretical work of Garibay-Alonso *et al.* (18). This type of self-organizing process, which we refer to as nanoparticle haloing, can be driven solely by repulsive interactions between such species in solution. We expect, however, that this process would be further enhanced by a weak attraction between the microspheres and nanoparticles, such as may arise from long-range van der Waals or locally induced electrostatic interactions (30).

The principal evidence for nanoparticle haloing around the silica microspheres is presented in Figs. 1 and 2. The ζ data reveal that the microspheres adopt a plateau value of $\approx$65 mV as the nanoparticle volume fraction in solution increases. This value is in agreement with the estimated ζ of the decorating nanoparticle species. The concentration dependence of ζ on ϕ_{nano} likely arises because nanoparticle haloing is regulated by two opposing processes: one stemming from the Coulombic repulsion between nanoparticles in the bulk solution (which drives their segregation) and the other stemming from a lateral Coulombic repulsion between nanoparticles in the halo region (which ultimately limits their distribution around the microspheres). The initial rise in ζ with ϕ_{nano} reflects the buildup of charged nanoparticles in the halo region, whereas the plateau in ζ occurs at higher ϕ_{nano} because of localized packing constraints that hinder additional nanoparticles from associating with the microspheres. Although this observed charge amplification could arise from nanoparticle adsorption, there was little evidence for this under the experimental conditions of interest. Assuming the data shown in Fig. 1*B* truly reflect nanoparticle adsorption, one would expect to measure an adsorption of 0.46 mg/m^2 at pH = 1.5 and $\phi_{nano} = 10^{-3}$ (which corresponds to a nanoparticle concentration in a solution of 3,650 mg/liter in Fig. 1*B*) via scanning angle reflectometry. Although this technique is clearly capable of resolving

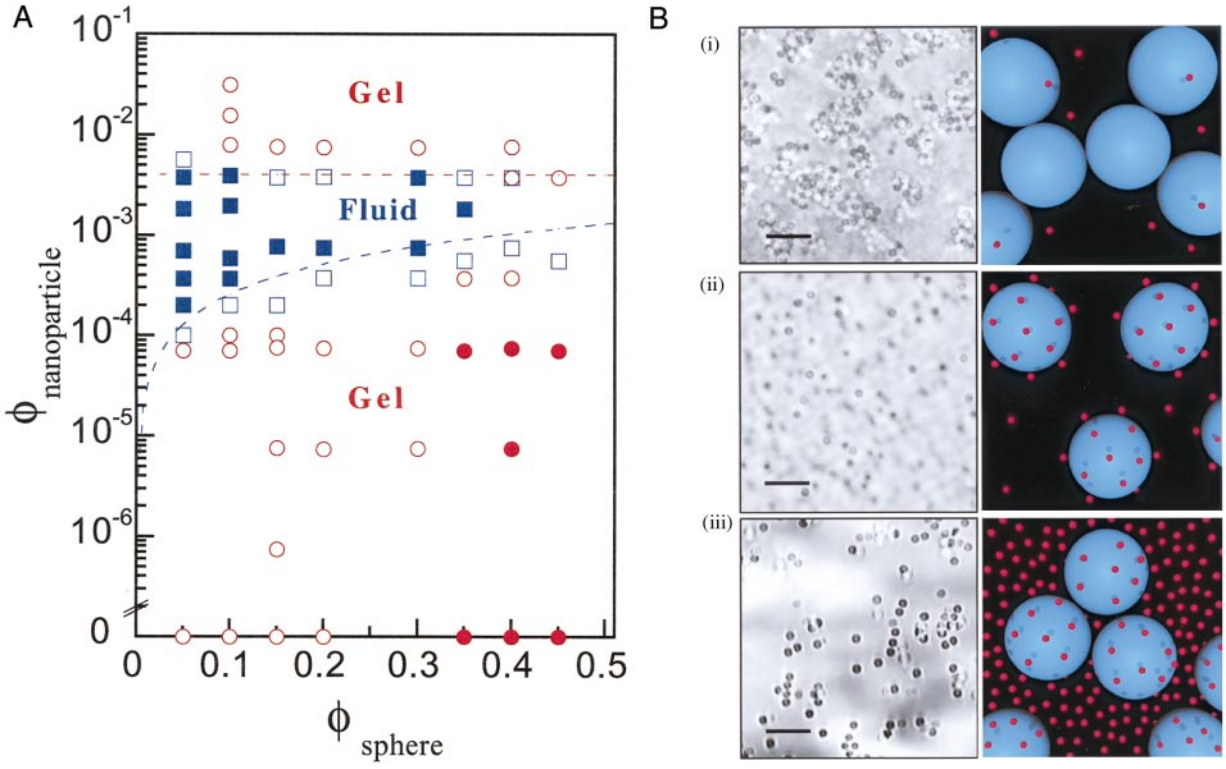

Fig. 3. (*A*) Phase diagram of mixtures of mutually attractive microspheres and repulsive nanoparticles (a_{micro} = 0.285 μm; a_{nano} = 3 nm) at pH = 1.5. ○, weak colloidal gel and a nanoparticle fluid; ●, colloidal gel and nanoparticle fluid; ■, homogeneous fluid; □, samples that have separated into a homogenous fluid and weak colloidal gel. Lower and upper dashed lines depict the experimentally observed lower ($\phi^{L,C}$) and upper ($\phi^{U,C}$) critical concentrations of nanoparticles, respectively. (*B*) Optical images and accompanying schematic illustrations of the phases in regions: (*i*) $\phi_{nano} < \phi^{L,C}$, (*ii*) $\phi^{L,C} \leq \phi_{nano} < \phi^{U,C}$, and (*iii*) $\phi_{nano} \geq \phi^{U,C}$. Optical micrographs (scale bar = 5 μm) correspond to samples prepared from dilute mixtures of larger microspheres (ϕ_{micro} = 0.001; a_{micro} = 0.590 μm) and nanoparticles. These conditions were selected to provide enhanced image clarity. Because of their size difference, only the microspheres are visible. The accompanying illustrations highlight the proposed distribution of microspheres (in blue) and nanoparticles (in red) in solution (their number density and size ratios are not drawn to scale).

nanoparticle adsorption of this magnitude (refer to Fig. 2*B*), we find no evidence of such phenomena at pH 1.5. Collectively, these data suggest only a weak interaction between the microspheres and nanoparticles, i.e., the highly charged nanoparticles residing near microsphere surfaces move cooperatively with the microspheres to give rise to their effective charge buildup and their reduction from the supernatant solution during microsphere sedimentation, but they are not strongly adsorbed. The origin of this weak interaction could stem solely from a Coulombic "pressure" exerted on the haloing nanoparticle species from their counterparts in the bulk solution or from a more complex, localized interaction that may arise between these highly charged species and the microspheres themselves.

Our observations provide a new method of generating charge on primary colloidal particles that contrasts sharply with the traditional approach of tailoring solvent pH well away from their isoelectric point (31). For the proposed mechanism, we can estimate the degree of nanoparticle segregation (or haloing) near the silica microsphere surfaces from the data shown in Fig. 1. The microsphere zeta potential plateaus at $\phi_{nano} \approx 0.003$ (i.e., a bulk nanoparticle concentration in solution of 10,950 mg/liter). A curve fit of the data plotted in Fig. 1*B* yields an association of $\approx$1 mg of nanoparticles/m^2 silica at this plateau concentration. Here, these data are normalized by microsphere surface area because the separation distance between the associated nanoparticles and the underlying microsphere surface is unknown. The effective nanoparticle radius a_{eff}, which accounts for their hard core radius and soft electrostatic double layer, is roughly a_{nano} + 3 nm, as determined from interparticle potential energy calculations by using the Derjaguin–Landau–Verwey–Overbeek theory (31). Assuming such species adopt a two-dimensional cubic array whose center-to-center separation distance ($2a_{eff}$) is governed by lateral (Coulombic) repulsive forces, we estimate a maximum halo concentration of 2.9 mg of nanoparticles/m^2 silica, close to the plateau value of $\approx$1 mg of nanoparticles/m^2 silica. Following this analysis, one finds that the predicted $\phi^{L,C}$ dependence on microsphere volume fraction (lower dashed line, Fig. 3*A*) is in good agreement with experimental observations.

Entropic Flocculation of Colloidal Microspheres. The origin of microsphere reflocculation at nanoparticle volume fractions above $\phi^{U,C}$ is explained by the rigorous force-balance depletion model developed by Walz and Sharma (16). Their model accounts for intensified depletion interactions stemming from the presence of highly charged species in solution. Flocculation of colloidal systems generally requires an attractive interaction of a few kT in magnitude. Piech and Walz have calculated an attractive depletion potential of roughly $-3\,kT$ for our system when ϕ_{nano} = 0.004 (M. Piech and J. Y. Walz, unpublished data). This value corresponds to $\phi^{U,C}$ depicted by the upper dashed line in Fig. 3*A*, which again is in good agreement with experimental observations. The traditional depletion mechanism can therefore only account for the observed reflocculation, not the remarkable stabilization at lower nanoparticle volume fractions.

Implications on Complex Fluid Behavior. Nanoparticle engineering of colloidal stability is not limited to systems of low pH, such as the one studied here. The salient feature of our approach is that

the colloidal microspheres are negligibly charged (be they suspended near their isoelectric point or surface functionalized with appropriate neutral groups), whereas the nanoparticles are highly charged (either positively or negatively) under the pH conditions of interest. Our observations therefore have broad impact on complex fluid behavior. Nanoparticle species can serve as multifunctional additives, providing the necessary stability for colloidal assembly as well as enhanced performance for a given technological application (1, 32). As an example, we observed that nanoparticle-stabilized silica microspheres assembled into colloidal crystals under gravity-driven sedimentation. Such systems may find application as templates for photonic materials (6, 33, 34), where incorporation of nanoparticles of high refractive index could yield enhanced dielectric contrast at the colloid-solution interface. Nanoparticle-stabilized fluids may also serve as inks for direct write technologies (3, 35) and drug delivery materials (10, 11) as well as precursors for novel coatings (36) and composites. Finally, nanoparticle agents may play an important role in tailoring the stability and, hence, phase transitions of complex biological fluids, e.g., protein-based systems (37–39).

Conclusions. We have demonstrated a fundamentally new mechanism for regulating the effective charge and, hence, stability of colloidal particles. We have shown that nanoparticle haloing, which could be driven solely by highly repulsive interactions between nanoparticles in solution, can generate a substantial ζ on colloidal microspheres suspended near their isoelectric point. For highly charged nanoparticles, this type of charge amplification can occur at extremely low nanoparticle volume fractions ($<10^{-3}$). This opens up a yet unexplored approach for achieving stabilization of attractive systems. Such phenomena are likely to be quite general and, thus, have important implications for complex fluids and their technological applications.

We thank P. Wiltzius, K. Schweizer, S. Granick, K. Suslick, C. Zukoski, and C. Martinez for discussions; J. Cesarano and R. Tilton for their help with experimental measurements; and M. Piech and J. Walz for help with depletion calculations. P.V.B. acknowledges partial support from the Department of Energy, Division of Materials Sciences through the Frederick Seitz Materials Research Laboratory, University of Illinois at Urbana-Champaign. This work was supported by the National Science Foundation (Grant NSF DMR-OO-71645) and the National Aeronautics and Space Administration Microgravity Research Program (Grant NAG8-1471).

1. Lewis, J. A. (2000) *J. Am. Ceram. Soc.* **83,** 3241–3259.
2. Agarwal, N. & Farris, R. J. (2000) *Polym. Eng. Sci.* **40,** 376–390.
3. Chrisey, D. B. (2000) *Science* **289,** 879–881.
4. Yablonovitch, E. (1987) *Phys. Rev. Lett.* **58,** 2059–2062.
5. Joannopoulos, J. D., Villeneuve, P. R. & Fan, S. (1997) *Nature (London)* **386,** 143–149.
6. Braun, P. V. & Wiltzius, P. (1999) *Nature (London)* **402,** 603–604.
7. Pan, G., Kesavamoorthy, R. & Asher, S. A. (1997) *Phys. Rev. Lett.* **78,** 3860–3863.
8. Johnson, S. A., Olivier, P. J. & Mallouk, T. E. (1999) *Science* **283,** 963–965.
9. Burmeister, F., Schäfle, C., Matthes, T., Böhmisch, M., Boneberg, J. & Leiderer, P. (1997) *Langmuir* **13,** 2983–2987.
10. Garnett, M. C., Stolnick, S., Dunn, S. E., Armstrong, I., Ling, W., Schacht, E., Ferutti, P., Vert, M., Davies, M. C., Illum, L. & Davis, S. S. (1999) *Mater. Res. Soc. Bull.* **24,** 49–56.
11. Muller, R. H. (1991) in *Colloidal Carriers for Controlled Drug Delivery and Targeting: Modification, Characterization, and In Vivo Distribution* (CRC, Boca Raton, FL).
12. Asakura, S. & Oosawa, F. (1958) *J. Polymer Sci.* **33,** 183–192.
13. Vrij, A. (1976) *Pure Appl. Chem.* **48,** 471–483.
14. Joanny, J. F., Leibler, L. & de Gennes, P. G. (1979) *J. Polym. Sci. Polym. Phys. Ed.* **17,** 1073–1084.
15. Gast, A. P., Hall, C. K. & Russel, W. B. (1983) *Faraday Discuss. Chem. Soc.* **76,** 189–201.
16. Walz, J. Y. & Sharma, A. (1994) *J. Colloid Interface Sci.* **168,** 485–496.
17. Nguyen, T. T., Grosberg, A. Y. & Shklovskii, B. I. (2000) *Phys. Rev. Lett.* **85,** 1568–1571.
18. Garibay-Alonso, R., Mendez-Alcaraz, J. M. & Klein, R. (1997) *Physica A (Amsterdam)* **235,** 159–169.
19. Ferreira, P. G., Dymitrowksa, M. & Belloni, L. (2000) *J. Chem. Phys.* **113,** 9849–9862.
20. Sperry, P. R. (1982) *J. Colloid Interface Sci.* **87,** 375–384.
21. Jenkins, P. & Snowden, M. (1996) *Adv. Colloid Interface Sci.* **68,** 57–96.
22. Liang, W., Tadros, T. F. & Luckham, P. F. (1993) *J. Colloid Interface Sci.* **158,** 152–158.
23. Peyre, V., Spalla, O., Belloni, L. & Nabavi, M. (1997) *J. Colloid Interface Sci.* **187,** 184–200.
24. Miller, K. T. & Zukoski, C. F. (1994) *J. Am. Ceram. Soc.* **77,** 2473–2478.
25. Flickinger, G. L. (1997) *The Gelation Behavior of Zirconia Sols* (Univ. of Illinois, Urbana-Champaign, IL).
26. Gisler, T., Schulz, S. F., Borkovec, M., Sticher, H., Schurtenberger, P., D'Aguanno, B. & Klein, R. (1994) *J. Chem. Phys.* **101,** 9924–9936.
27. Furst, E. M., Pagac, E. S. & Tilton, R. D. (1996) *Ind. Eng. Chem. Res.* **35,** 1566–1574.
28. Pagac, E. S., Tilton, R. D. & Prieve, D. C. (1998) *Langmuir* **14,** 5106–5112.
29. Pusey, P. N. & van Megen, W. (1986) *Nature (London)* **320,** 340–342.
30. Miklavic, S. J., Chan, D. Y. C. & White, L. R. (1994) *J. Phys. Chem.* **98,** 9022–9032.
31. Hunter, R. J. (1995) *Foundations of Colloid Science* (Clarendon, Oxford), Vols. 1 & 2.
32. Guo, J. J. & Lewis, J. A. (1999) *J. Am. Ceram. Soc.* **82,** 2345–2358.
33. Biswas, R., Sigalas, M. M., Subramania, G. & Ho, K.-M. (1998) *Phys. Rev. B* **57,** 3701–3705.
34. Blaaderen, A. V. (1998) *Mater. Res. Soc. Bull.* **23,** 39–43.
35. Morissette, S. L., Lewis, J. A., Cesarano, J., Dimos, D. B. & Baer, T. (2000) *J. Am. Ceram. Soc.* **83,** 2409–2416.
36. Burmeister, F., Schäfle, C., Keilhofer, B., Bechinger, C., Boneberg, J. & Leiderer, P. (1998) *Adv. Mater.* **10,** 495–497.
37. Durbin, S. D. & Fehrer, G. (1996) *Annu. Rev. Phys. Chem.* **47,** 171–204.
38. ten Wolde, P. R. & Frenkel, D. (1997) *Science* **277,** 1975–1978.
39. Rosenbaum, D., Zamora, P. C. & Zukoski, C. F. (1996) *Phys. Rev. Lett.* **76,** 150–153.